https://doi.org/10.5194/bg-2023-146
Preprint. Discussion started: 28 September 2023

Biogeosciences Discussions

The Southern Ocean as the freight train of the global climate under zero-emission scenarios with ACCESS-ESM1.5

Matthew A. Chamberlain[a], Tilo Ziehn[b], and Rachel M. Law[b]

[a]CSIRO Environment, Hobart, TAS, Australia
[b]CSIRO Environment, Aspendale, VIC, Australia

Correspondence: Matthew A. Chamberlain (matthew.chamberlain@csiro.au)

Abstract.

Climate projection experiments presented here explore how the slow response in the Southern Ocean drives ongoing global warming even with zero CO_2 emissions and declining atmospheric CO_2 concentrations. These projections were simulated by the Earth System Model version of Australian Community Climate and Earth System Simulator (ACCESS-ESM1.5) and motivated by the Zero Emission Commitment Multi-model Intercomparison Project. ZECMIP simulations branch from the idealised warming with the "1-percent CO_2" CMIP experiment onto a trajectory of zero carbon emissions. The original ZECMIP experiments simulated the zero-emission trajectories after emitting 1000 Pg of carbon into the climate, and optionally 750 and 2000 PgC; here we show extra trajectories after 1250, 1500 and 1750 PgC, and simulate climates to 300 years after branching to demonstrate long-term trends. In each of these experiments that switch to zero emissions after emitting 1000 PgC or more, the global climate continues to warm. In the case of the experiment that branched after 2000 PgC, or after 3.5°C of warming from a pre-industrial climate, there is 0.37°C of extra warming after 50 years of zero emissions and further warming continues for at least several centuries.

From early in the 1-percent CO_2 experiment, the circulation of the Southern Ocean is modified by the warming climate which drives changes in the distribution of both physical and biogeochemical subsurface ocean tracers that are ongoing in all zero-emission branches.

We replicate the global climate warming in 1-percent CO_2 and ZECMIP experiments with a simple slab model that contains regions that respond with different time scales to atmospheric CO_2 and climate forcing, demonstrating the global climate response is due primarily to the slow response of the ocean, the Southern Ocean in particular. In these zero emission trajectories, the simulated climate moves from a Transient Climate Response (TCR) state towards a Equilibrium Climate Sensitivity (ECS) state. Since ECS is substantially greater than TCR, the global temperature can increase while CO_2 decreases.

https://doi.org/10.5194/bg-2023-146
Preprint. Discussion started: 28 September 2023


Biogeosciences Discussions Open Access EGU

1 Introduction

The Zero-Emission Commitment (ZEC) of the global climate is defined as the amount of warming that would occur after the cessation of anthropogenic CO_2 emissions (Matthews and Weaver, 2010). The ZEC is one of the critical terms in the calculation of the potential budget of carbon emissions permitable without exceeding any agreed thresholds of "safe" warming (Rogelj et al., 2019); other terms being the amount of historical warming, the transient climate response to ongoing emissions, warming due to non-CO_2 greenhouse gases and corrections for climate feedbacks.

In recent assessments of the remaining carbon emission budgets, the value of ZEC has typically been assumed to be zero (e.g., Rogelj et al., 2018). The reasoning has been that after the cessation of carbon emissions, the existing carbon in the climate system will redistribute between the atmosphere, land and ocean, reducing the atmospheric CO_2 and have a cooling effect on the climate. On the other hand, a slow down in planetary heat uptake (into the ocean in particular) will have a warming effect, largely cancelling so that the net result of ZEC has been assumed to be close to zero (Rogelj et al., 2019). This conclusion had been based largely on results from limited climate simulations.

In order to reduce the uncertainty associated with this ZEC contribution, a ZEC Model Intercomparison Project (ZECMIP) was designed (Jones et al., 2019) with experiments to simulate climate responses under zero emission scenarios, branching after varying total emission budgets of CO_2. Experiments under ZECMIP explore idealised zero emission climate trajectories. The Earth System Model version of Australian Community Climate and Earth System Simulator (ACCESS-ESM1.5) submitted results for type-A ZECMIP experiments, which branch from the *1pctCO2* which is one of the core Coupled Model Intercomparison Project (CMIP) experiments. In *1pctCO2* the climate state warms with prescribed atmospheric CO_2 that increases by 1% per year, for 140 years. Only atmospheric CO_2 is modified and all other forcings (e.g., from aerosols and CH_4) remain at prescribed preindustrial levels. As such, ZECMIP projections represent idealised zero-emission simulation that are insightful to climate responses to possible future scenarios.

Many of the Earth System Models (ESMs) that contributed to version 6 of CMIP (Eyring et al., 2016) also participated in ZECMIP, including the ACCESS-ESM1.5, as presented in MacDougall et al. (2020). Of the four full ESMs that submitted results for all three ZECMIP-A experiments (branching after the emission of 750, 1000 and 2000 PgC), two ESMs simulated warmer global temperatures 50 years into the high ZECMIP branch (UKESM1 and ACCESS-ESM1.5) and two ESMs simulated cooling (MIROC-ES2L and GFDL-ESM2M).

In this paper, we investigate the evolution of the climate state within the ZEC experiments with extra experiments. In the initial results submitted to ZECMIP, ACCESS-ESM1.5 only continued to warm in the high branch that started after the emission of 2000 Pg of carbon. Low branches, starting after 750 and 1000 PgC, showed a small cooling to neutral responses. We use extra experiments, presented here, branching at intermediate points between the 1000 and 2000 PgC branches to better evaluate the ongoing changes as the climate stabilises. Section 2 describes the model and summarises the experiments. Section 3 presents the results: time series of global metrics, trajectories of surface temperatures, changes in the ocean circulation and tracer distributions, and, the trajectories of the various ZEC branches with respect to average CO_2 and temperature. Section 4 presents

https://doi.org/10.5194/bg-2023-146
Preprint. Discussion started: 28 September 2023


Biogeosciences Discussions Open Access EGU

a simple climate inertia model that replicates the time series of ACCESS-ESM1.5 global averages and compares results with other ESMs submitted to ZECMIP. Section 5 summarises the work.

2 Method

2.1 Model Description

The ACCESS-ESM1.5 participated in CMIP6, a global effort to coordinate the design and comparison of climate models and their simulations, and submitted output to several endorsed model intercomparison projects (Mackallah et al., 2022). The model is described in detail in Ziehn et al. (2020). In brief, the atmospheric model is the UK Met Office Unified Model (UM, version 7.3, The HadGEM2 Development Team: et al., 2011) configured with N96 resolution ($1.875°$ longitude and $1.25°$ latitude resolution) and 38 vertical levels, which is coupled to a nominally $1°$ resolution ocean model Modular Ocean Model (MOM Version 5, Griffies, 2012) and CICE sea ice model (version 4.1, Hunke and Lipscomb, 2010).

Biogeochemical components of the ACCESS-ESM1.5 are Community Atmosphere Biosphere Land Exchange (CABLE, Kowalczyk et al., 2013) and World Ocean Model of Biogeochemistry And Trophic-dynamics (WOMBAT, Oke et al., 2013; Law et al., 2017). CABLE in ACCESS-ESM1.5 is enabled with carbon-nitrogen-phosphorous cycles. The implementation of phosphorous is unique in ACCESS-ESM1.5 and is discussed in Ziehn et al. (2021). WOMBAT is a phosphorous-based nutrient-phytoplankton-zooplankton-detritus model. Both CABLE and WOMBAT include carbon cycles enabling an active carbon-cycle in ACCESS-ESM1.5 and the capability to execute these simulations of zero emission scenarios.

In the development of ACCESS-ESM1.5 from the previous version (ACCESS-ESM1.0, Law et al., 2017) the biases in the physical and biogeochemical states have been reduced and model has been run for 1000s of years. In the control experiment forced with constant preindustrial conditions (*piControl*), trends and biases are small in the physical ocean (-8.5x10^{-5} °C century^{-1} in average sea surface temperature) and biogeochemistry (land and ocean carbon fluxes were 0.02 and -0.08 PgC year^{-1} respectively), as reported in Ziehn et al. (2020). This stable state makes the model and the base climate highly suitable for studying climate processes and long term responses to various changes in climate forcing.

2.2 Supplementary zero emission experiments

The work presented here includes new versions of experiments based on the original ZECMIP branches from the *1pctCO2*, as well as three extra experiments from intermediate branch points (Table 1) that were designed to understand the transition in the climate response between “low” and “high’ ZEC branches. All these experiments were integrated for 300 years from the branch point to investigate long term changes within the climate system that can be obscured by variability in shorter integrations. These new experiments were executed with the same configuration as the original branches. However, these experiments were run on updated computer hardware, so while the results are equivalent to the original ZECMIP submission, they are not identical. Hence, values in Table 1 are not the same as those submitted to ZECMIP; differences are only due to the internal variability of the model. Note also, the parent *1pctCO2* experiment was also repeated on the new computer and

https://doi.org/10.5194/bg-2023-146
Preprint. Discussion started: 28 September 2023

Biogeosciences Discussions Open Access EGU

Table 1. List of ZECMIP-style experiments with ACCESS-ESM1.5 presented here: the year each experiment branches from *1pctCO2* that started in year 0101, the anomaly of the 20-year averaged *1pctCO2* global temperature centred at the branch point with respect to *piControl*, and, the change in 20-year averaged temperatures at 25, 50, 100 and 200 years in each ZEC experiment with respect to its branch point. Branches that repeat experiments submitted to ZECMIP are indicated (*); values are from the new experiments presented here. As a measure of the uncertainty in these values, the standard deviation in the 20-year averaged temperatures from *piControl* is 0.06°C.

Carbon emitted (PgC)	Model Year	ΔT	ZEC_{25}	ZEC_{50}	ZEC_{100}	ZEC_{200}
750*	0154	1.39	0.05	-0.06	-0.10	-0.10
1000*	0168	1.82	0.02	0.01	0.02	-0.02
1250	0181	2.20	0.14	0.31	0.17	0.20
1500	0194	2.61	0.28	0.34	0.44	0.53
1750	0205	3.10	0.24	0.34	0.47	0.58
2000*	0216	3.51	0.33	0.37	0.57	0.83

this version is the parent experiment to the results presented. Table 1 lists the branch points, the year of the *1pctCO2* and the average global temperature at the branch point, relative to pre-industrial.

Low (high) ZEC branches depart from *1pctCO2* after relative low (high) budgets of emitted carbon on the *1pctCO2* trajectory. Note that the *1pctCO2* experiment is a "concentration-driven" experiments with a prescribed atmospheric content of CO_2, increasing 1% each year, and these budgets of carbon emissions into the climate are diagnosed from land and ocean fluxes. When transitioning onto any ZEC branch, the model switches to an "emission-driven" experiment, allowing the active carbon cycle to determine the exchange between climate components, conserving the global carbon content and determining the atmospheric CO_2 concentration based on these exchanges.

In ZECMIP experiments, all non-CO_2 "greenhouse gases" and aerosols are held constant, and likewise land use and vegetation type maps are maintained with preindustrial distributions. This series of idealised zero-emission experiments are quite different to plausible climate scenarios for the 21st century in which other gases and aerosols are also influencing the climate, and a global instantaneous transition to zero carbon emissions is also unrealistic. However, the processes simulated in these ZECMIP-style experiments are useful for insights into plausible future climate responses, and results can be readily related to other more realistic stabilisation scenarios by comparing corresponding branch point temperatures.

3 Results

The first subsection below presents globally-averaged time series, demonstrating the range of the responses from the full series of ZEC experiments, from low branches where the climate states recovers somewhat from the rising temperatures of the parent *1pctCO2* experiment, to high branches in which climate state continues to warm despite decreasing atmospheric CO_2. The next subsection shows changes in surface temperatures to understand what regions drive the ongoing changes seen in high

https://doi.org/10.5194/bg-2023-146
Preprint. Discussion started: 28 September 2023

ZEC branches. The third subsection characterises the changes in the circulation and distribution of tracers within the Southern Ocean that are associated with ongoing global warming the in high ZEC branches. The final subsection tracks the trajectory of ZEC branches with respect to atmospheric CO_2 and temperature.

3.1 Global metrics

Figure 1 shows time series of several globally averaged climate metrics from *1pctCO2* and ZEC branches, along with the *piControl*. The time series of temperatures from each ZEC branch is about linear and the gradients increase evenly from -0.035°C/100y in *ZEC750* to +0.315°C/100y in *ZEC2000* (Fig. 1a), with no clear tipping point or step change in the ZEC branch responses. As expected, atmospheric CO_2 concentrations drop in all ZEC branches but remain well above preindustrial values (Fig. 1b). Due to the slow response of the deep ocean and the persistent high atmospheric CO_2 values, ocean heat continues to increase in all ZEC branches (Fig. 1c), in the case of high branches, the ongoing oceanic heat uptake is close to the uptake in *1pctCO2* with increasing CO_2 forcing. The rate of the oceanic heat uptake is the main component of the energy imbalance at the top of the atmosphere (TOA) in all experiments (Fig. 1d). In the case of *piControl*, the non-zero TOA balance is consistent with the offset noted in Ziehn et al. (2020). The response of sea ice areas in the Arctic and Antarctic in the ZEC branches are distinct (Figs. 1e and 1f respectively). The Arctic sea ice area largely follows the changes of average global surface temperature (Fig. 1a). On the other hand, the Antarctic sea ice is largely unresponsive in the start of the *1pctCO2* and even the first 100 years of low ZEC branches. However, the longer integrations of the ZEC experiments presented here show reductions in Antarctic sea ice even in the *ZEC750* branch, where after 200 years sea ice area is outside the range of values from the *piControl*. The initial sea ice trajectory of *ZEC2000* is close to that of *1pctCO2*, indicating that the trajectory of the sea ice here at this time is already "locked in" and independent of atmospheric forcing for several decades.

3.2 Surface temperature changes

Figure 2 shows the evolution in zonally averaged near-surface temperatures in the *1pctCO2* and selected ZECMIP experiments. In *1pctCO2* there is a strong dominant warming in the Arctic responding to the increased climate forcing from higher atmospheric CO_2 (Fig. 2a). However, the Arctic also cools as the atmospheric CO_2 decreases in low ZEC branches (Fig. 2b). The Arctic surface temperature changes appear to follow changes in the global temperature with local amplification from ice albedo feedback. In contrast, the Southern Ocean warms relatively slowly in *1pctCO2* and yet continues to warm in all ZEC branches, consistent with being the region with the greatest inertia in the climate system. For instance, while there is an overall global cooling in *ZEC750*, the extension of this experiment shows warming of ~ 1°C, on average, in a latitude band of $40 - -65°$ S, 200 years after branching from *1pctCO2* (Fig. 2b). At $65 - -70°$ S, the magnitude of warming in low ZEC branches is about the same as warming north 60° S, whereas these poleward latitudes clearly dominate the warming in *ZEC2000* corresponding to strong decreases in Antarctic sea ice area as seen in Fig. 1f.

Figure 3 shows the spatial distribution of the temperature changes of *1pctCO2* and ZEC branch experiments, calculated here as the difference between the last and first decade from within each branch or experiment. In low ZEC branches (Fig. 3b and c) there is a broad Southern Ocean response that shows warming across the Atlantic and Indian sectors, extending north to

https://doi.org/10.5194/bg-2023-146
Preprint. Discussion started: 28 September 2023

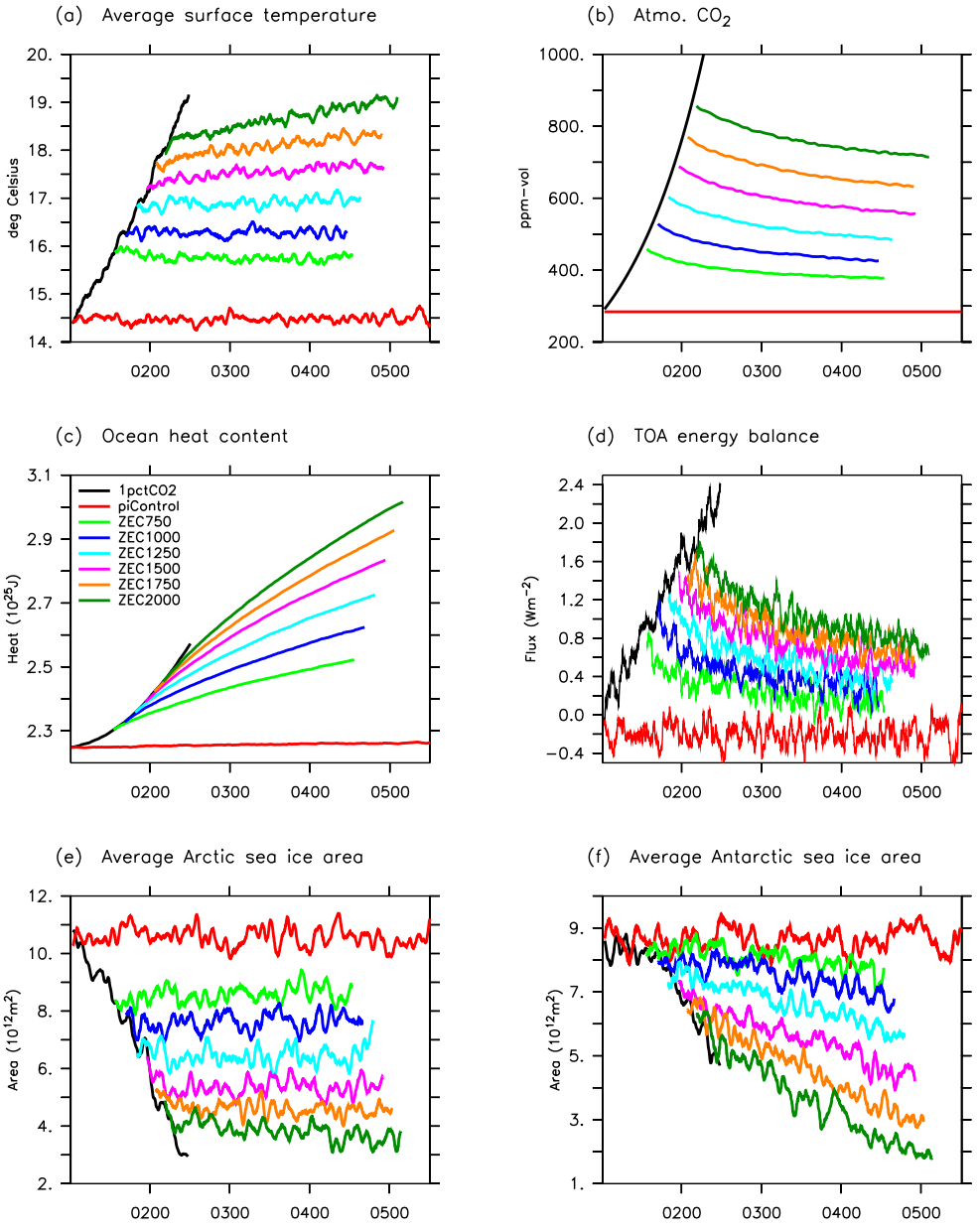

Figure 1. Global time series of (a) average near-surface temperature, (b) atmospheric CO_2, (c) ocean heat content, (d) top-of-atmosphere energy balance, and sea ice area of the (e) Arctic and (f) Antarctic from the *1pctCO2* and ZEC branches and the *piControl*. Time series are smoothed with 5-year running averages.

https://doi.org/10.5194/bg-2023-146
Preprint. Discussion started: 28 September 2023

Biogeosciences
Discussions
Open Access
EGU

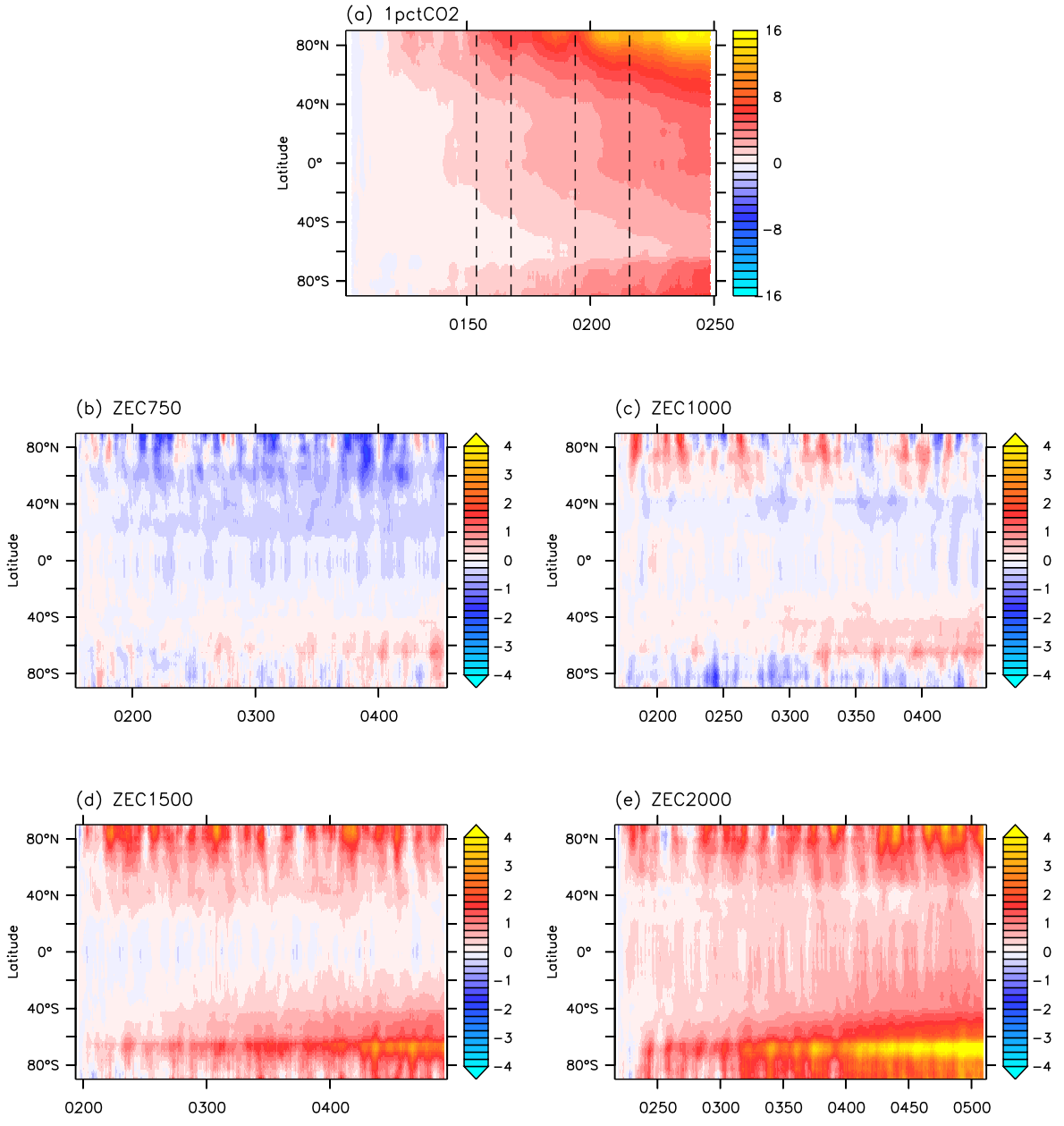

Figure 2. Changes in zonally averaged surface temperatures with time from *1pctCO2* and four of the ZEC branches investigated here. Differences are with respect to the average of the first 10 years of each experiment, and smoothed with a 5-year filter. Dashed vertical lines in (a) indicate times that the ZEC branches shown leave *1pctCO2*.

https://doi.org/10.5194/bg-2023-146
Preprint. Discussion started: 28 September 2023

$\sim 45^\circ$ S, though not in the Pacific sector which is about neutral. High ZEC branches (Fig. 3d and e) show larger magnitudes of warming in the Southern Ocean that then drive global changes (note the expanding influences in the zonal time series, Fig. 2d and e). Warming is still evident across the broad regions of the Southern Ocean, but now the greatest temperature change is located in sea ice regions south of 60° S where changes now trigger positive ice feedbacks.

It is evident that neutral global responses of lowest branches in Fig. 1 obscure significant regional changes. In particular, Fig. 2 and Fig. 3 demonstrate ongoing warming of the order of 1°C over the Southern Ocean that is largely compensated by cooling over large continental regions in low ZEC branches. In high ZEC branches, the change in temperature in these continental regions is small with respect to ocean and the Southern Ocean in particular. While there may still be some locations of cooling with decreasing atmospheric CO_2, the cooling is significantly less relative to the cooling in low ZEC branches. Also, cooling in these high branches is only found at locations within large continental areas. In contrast, Australia as a smaller continent tends to warm with the neighbouring oceans. Interestingly, one oceanic region shows less warming, and even some cooling in *ZEC1500* and *ZEC2000*, around the northern subtropical Pacific which is relatively isolated to warming trends in Arctic or Southern Ocean.

3.3 Subsurface changes

3.3.1 Overturning

Sections of global meridional overturning from different stages of *1pctCO2* are shown in Fig. 4. Overturning sections are shown with respect to depth and density coordinates, and both indicate a decline in strength of circulation of Antarctic Bottom Water. There is a greater influence on the deep bottom water circulation at 3000–4000m in the second half of *1pctCO2* (the change in 4c to 4e being greater than 4a to 4c). The density of the circulation close to the Antarctic coast, south of 60° S, decreases over the course of *1pctCO2* (Fig. 4b, d and f), breaking the coupling to the bottom circulation across the rest of the global ocean. In sections of both coordinates, the Deacon Cell (55° S to 40° S) in the Southern Ocean is stronger and more extensive at the end of *1pctCO2*.

The times series of the overturning shown in the bottom row of Fig. 4 are calculated as the magnitude of the minimum in the streamfunction in depth coordinates at two latitudes, 72° S and 66° S. There is a lot of variability in these overturning values, but with 10-year averaging persistent changes in all ZEC branches become evident, exceeding the significant decadal variability. Even low ZEC branches demonstrate that the small perturbations in average overturning relative to *piControl* do not recover in the 300-year integrations of the branches. Overturning time series in high ZEC branches at 72° S (Fig. 4g) continue to evolve after branching from *1pctCO2* indicating the slow response of deep overturning to changes in surface boundary conditions.

Circulation time series at 66° S appears to collapse as calculated in depth coordinates in Fig. 4h. Average overturning at this position in *piControl* is $\sim$4 Sv, albeit with significant decadal variability with a range that is also $\sim$4 Sv, and drops to $\sim$1 Sv in the low ZEC branches and even < 0.5 Sv in high branches, with no indication of any recovery in the 300-year

https://doi.org/10.5194/bg-2023-146
Preprint. Discussion started: 28 September 2023

Biogeosciences
Discussions
Open Access
EGU

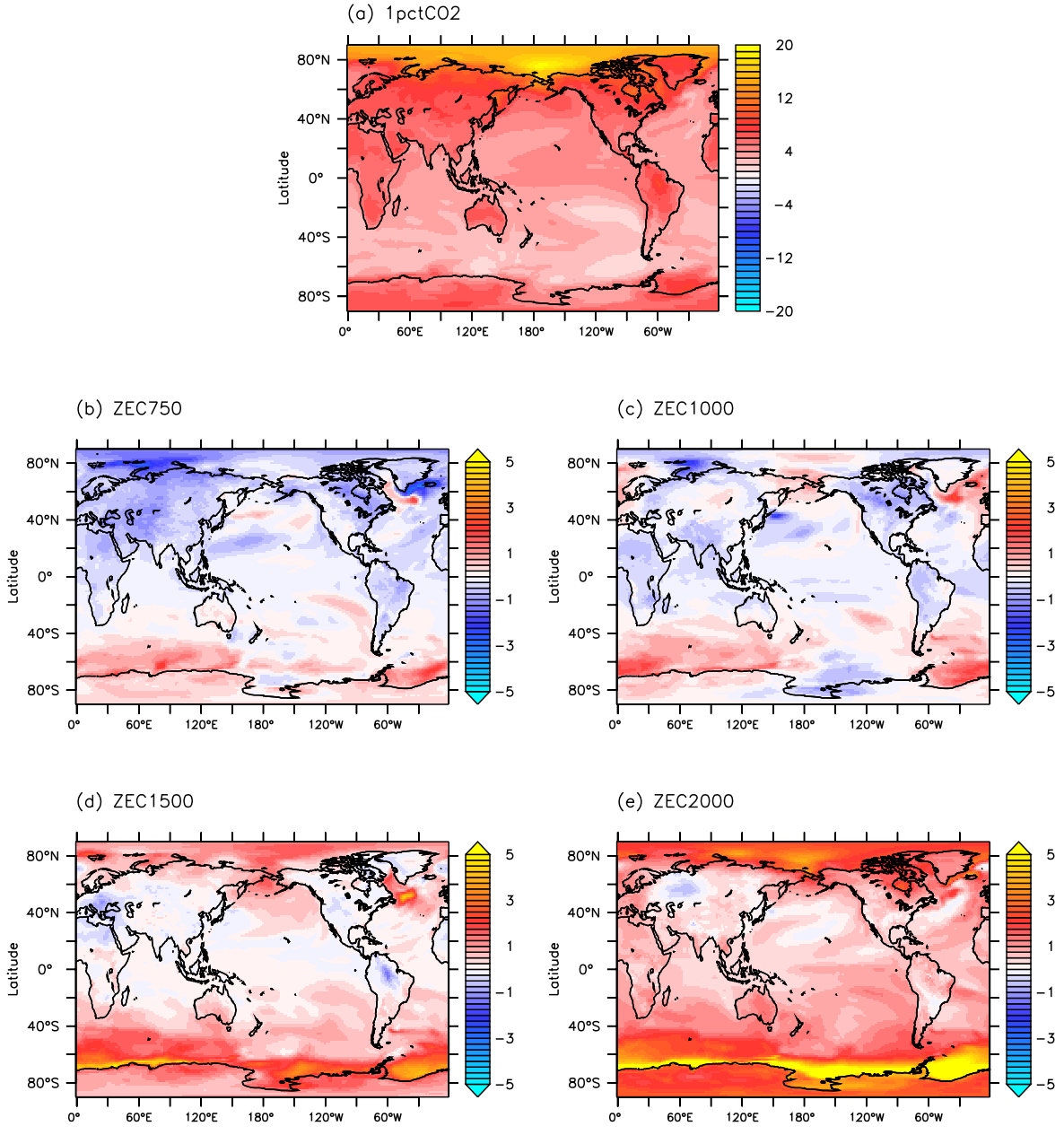

Figure 3. Change in surface temperatures, from averages of last and first decades of *1pctCO2* (time difference, Δt=140y) and four of the ZEC branches (Δt=290y).

https://doi.org/10.5194/bg-2023-146
Preprint. Discussion started: 28 September 2023

integrations. However, overturning sections in density coordinates indicate circulation is ongoing at these latitudes. The timing of the branching of the lowest ZEC branches is about the time that the cell south of 60° S starts to shift to light densities.

3.3.2 Tracer distributions

The changes in the circulation and surface forcing from the increased climate forcing of *1pctCO2* initiate long term changes in the distribution of subsurface ocean properties that continue even once the climate forcing decreases and stabilises in the ZECMIP experiments. Figures 5, 6 and 7 show changes in zonally averaged sections of temperature, salinity and oxygen in the *1pctCO2*, *ZEC750* and *ZEC2000*, as well as time series of tracers at selected positions from *1pctCO2*, *piControl* and all ZEC branches. Figure 8 demonstrates the changes in the ocean depth of heat uptake in the different ZEC branches.

The time series (panels i, j, and k of Fig.s 5, 6 and 7) demonstrate that even small circulation changes of low ZEC branches are sufficient to drive ongoing subsurface changes in heat, salt and oxygen, even if these changes are not expressed at the surface. There is a montonic increase in the rate of change in the subsurface warming with the ZEC branches, the slowest warming is in upper 100s of metres in the lowest ZEC branch and the fastest warming is in the interior of the thermocline, ∼500–1500 m in the highest branch. Similar responses are seen in oxygen time series (Fig. 7), where high branches generate greater decreases in oxygen. with exceptions that are discussed further below. For the time series of each tracer at 20° S (panel l of each figure), while there are consistent signals across the experiments presented, the magnitudes of low-frequency variability is similar to the these signals and a larger 30-year filter is applied to reduce this variability.

Changes in the temperature sections of *1pctCO2* (Fig. 5d and g) are predominately near the surface north of 40° S, with deeper warming near Antarctica down to 2000 m and in the Southern Ocean at 45–50° S down to 1000 m related to a poleward shift in water masses. In contrast, temperature changes in ZEC branches are predominantly at depth, ∼ 500–1500 m and deeper south of 60° S, with less change at the surface. North of 50° S, temperature changes are relatively uniform with latitude and these outcrop in the Southern Ocean.

The uptake of heat in *1pctCO2* and selected ZEC branches are shown in Fig. 8, as changes in the globally averaged temperature with depth and time within each experiment. Consistent with the ocean heat content in Fig. 1c, temperature increases are much larger in high ZEC branches; also, the distribution of temperature increase is shallower in high branches. At the end of the 300 years with zero emissions, the peak temperature increase in *ZEC2000* is ∼800 m whereas in *ZEC750* it is ∼1200 m. While temperature still increases below ∼200 m in *ZEC750*, there is some cooling in the upper 100 m in response to the decreasing atmospheric CO_2 and reduced climate forcing. In contrast, in *ZEC2000*, the highest temperature increase is closer to the surface and has a greater influence on the upper ocean and surface.

Figure 6 shows changes in zonal averages of salinity from *1pctCO2* and selected ZEC branches. The changes in zonal sections of salinity in *1pctCO2* vary spatially, with freshening in the upper ocean near Antarctica and increasing salinity below 800 m. In *ZEC750*, the main change in the salinity section is a freshening between 40 and 60° S in the upper 1000 m. In *ZEC2000* the ongoing salinity changes are more uniform, with a general freshening of the upper ocean above a band of increasing salinity below 500 m near Antarctica and extending north of 50° S at depths between 1000 and 2000 m.

https://doi.org/10.5194/bg-2023-146
Preprint. Discussion started: 28 September 2023

Changes in the distribution of salinity are somewhat slower to become evident in *1pctCO2*. For instance, in the time series for the positions shown in panels j, k and l of Fig. 6, the salinity differences between *ZEC750* and the control are minor even after 300 years. Trends in temperature at the same positions were more distinct from the control and showed growing differences after 300 years. The transient response of salinity at 25° S and 250 m in *1pctCO2* is an increase in salinity. However, in all ZEC branches salinity decreases, albeit with significant interannual variability, indicating a recovery in the atmospheric circulation and precipitation under zero-emission climates with decreasing atmospheric CO_2.

The distribution and responses of ocean biogeochemical tracers (for example oxygen, Fig. 7) are distinct from both heat and salinity, due to the different distributions of tracer sources and sinks, both at the ocean surface and in the interior. Hence, the mean fields of biogeochemical tracers are distinct from physical tracers and are impacted in different ways by the changes in ocean state and circulation. As the strength of the overturning Antarctic cells weaken, there is a decrease in the supply of oxygen from surface waters into all depths of the interior of Southern Ocean. Local exceptions to the general decline in oxygen include water between 0 and 1000 m at 50–60° S in low ZEC branches where oxygen likely increases due to the greater influence from southern oxygen-rich surface water and less from oxygen-poor waters because of changes in circulation and global stratification (panels e and h of Fig. 7). There is also an increase in subsurface oxygen below equatorial regions where productivity declines in warming climates. Reduced productivity and export of organic material reduce the consumption of subsurface oxygen in these regions driving this oxygen increase.

https://doi.org/10.5194/bg-2023-146
Preprint. Discussion started: 28 September 2023

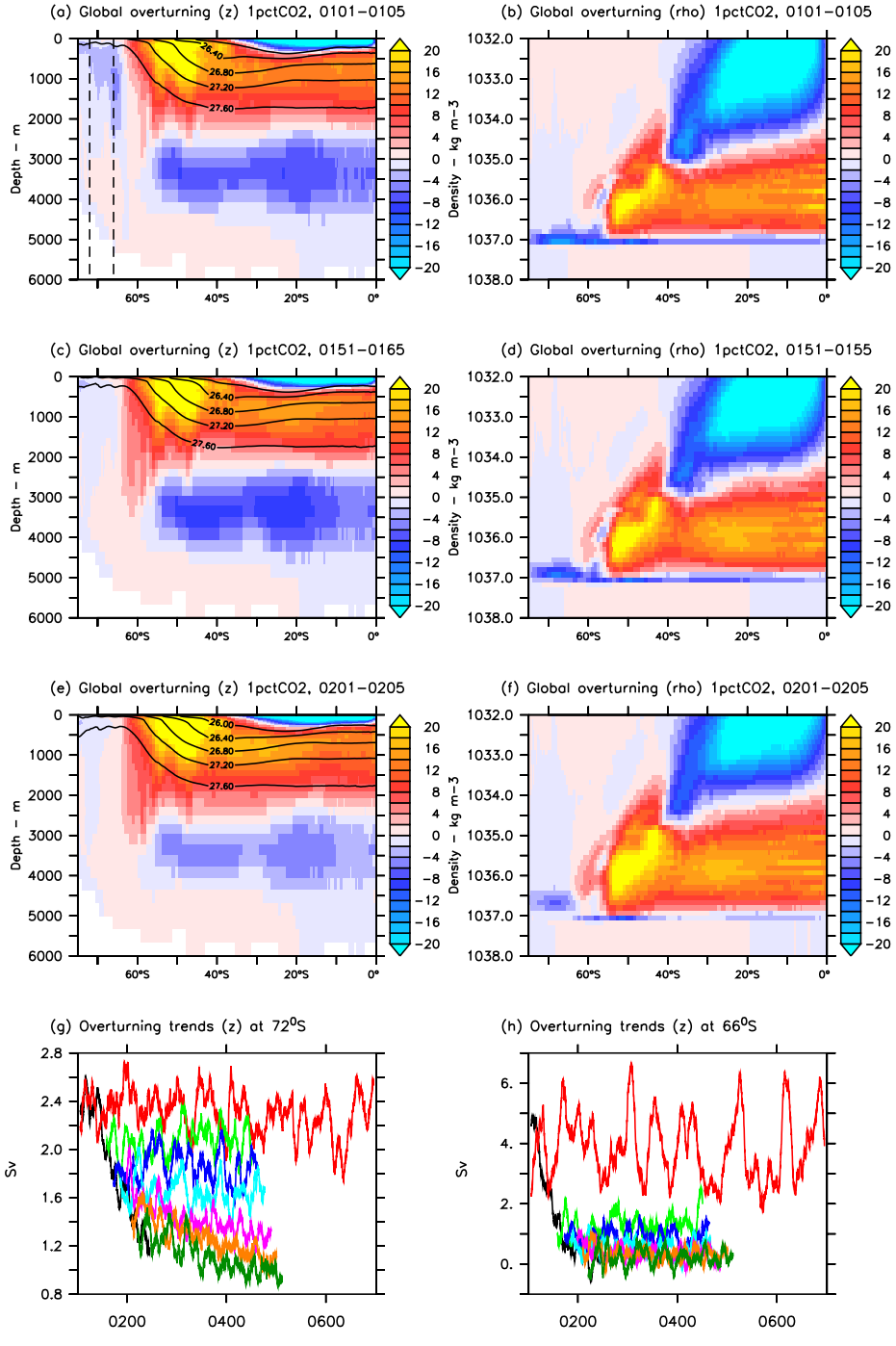

Figure 4. Global meridional overturning from *1pctCO2* calculated with respect to depth (left) and density (right, referenced to 2000 decibars). Sections show 5-year averages of overturning: first 5 years of *1pctCO2* (top row), years 50–54 (2nd row), and years 100–104 (3rd row). The bottom row show time series, of 10-year averages to reduce variability, in the strength of dense water circulation calculated with respect to depth at two positions near Antarctica (at 72° S and 66° S, indicated by dashed lines in top row), from *1pctCO2*, *piControl* and ZEC branches (using the same colour scheme as Fig. 1).

https://doi.org/10.5194/bg-2023-146
Preprint. Discussion started: 28 September 2023

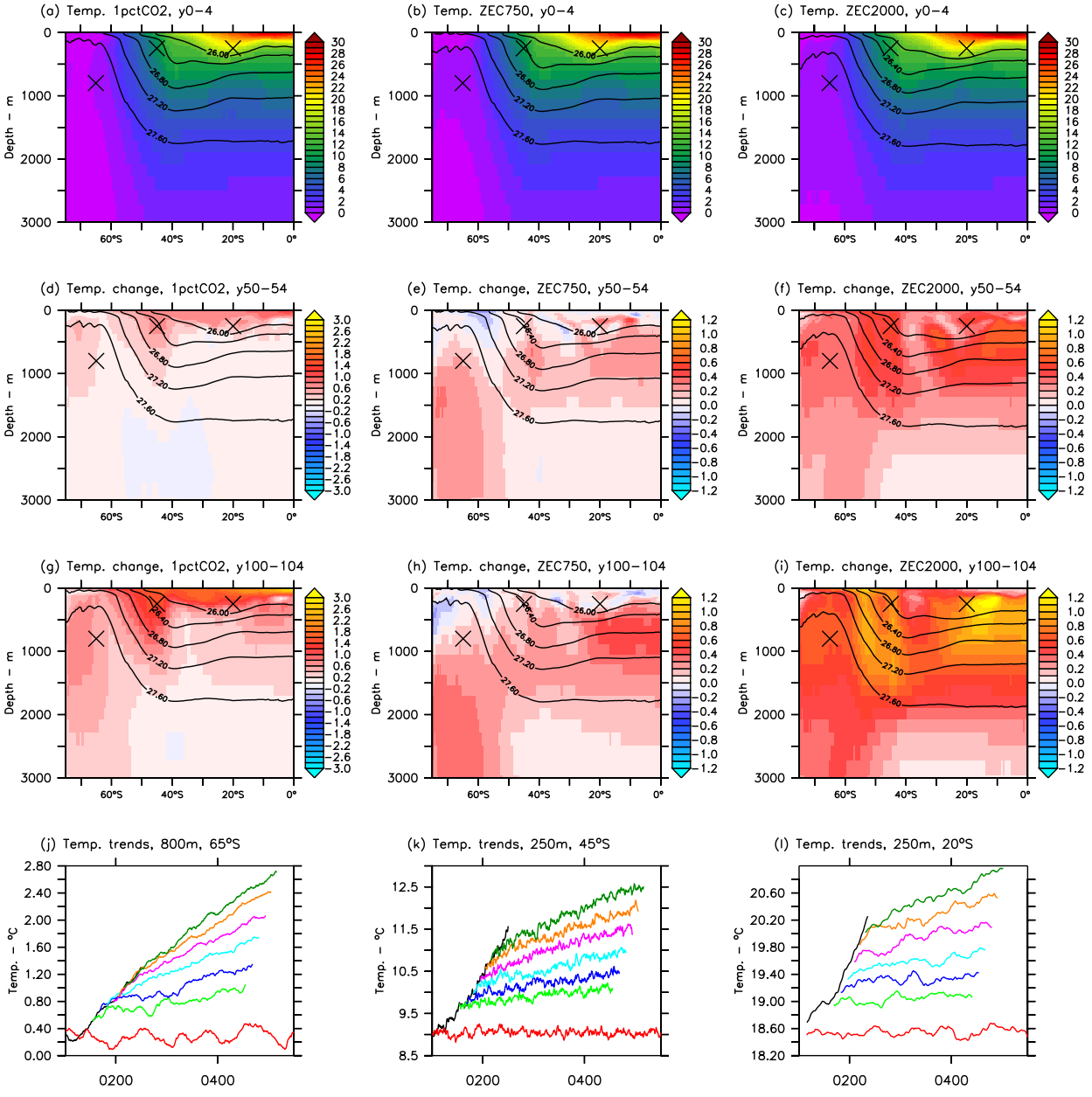

Figure 5. Changes and time series in average zonal sections of temperature. The top row shows zonally averaged sections for the first 5 years of from *1pctCO2* (left) and ZECMIP branches after emitting 750 PgC (middle) and 2000 PgC (right). The second and third rows show changes in zonally averaged sections from the same experiments after 50 and 100 years, respectively. Contours indicate zonally averaged potential densities. The bottom row show temperature trends in the subsurface of the Southern Ocean (at 65° S, 45° S and 20° S, at positions indicated), from *1pctCO2*, *piControl* and ZEC branches (same colour scheme as Fig. 1). Trends at 65° S and 45° S are filtered by 1 year, trends at 20° S are filtered by 30 years.

https://doi.org/10.5194/bg-2023-146
Preprint. Discussion started: 28 September 2023

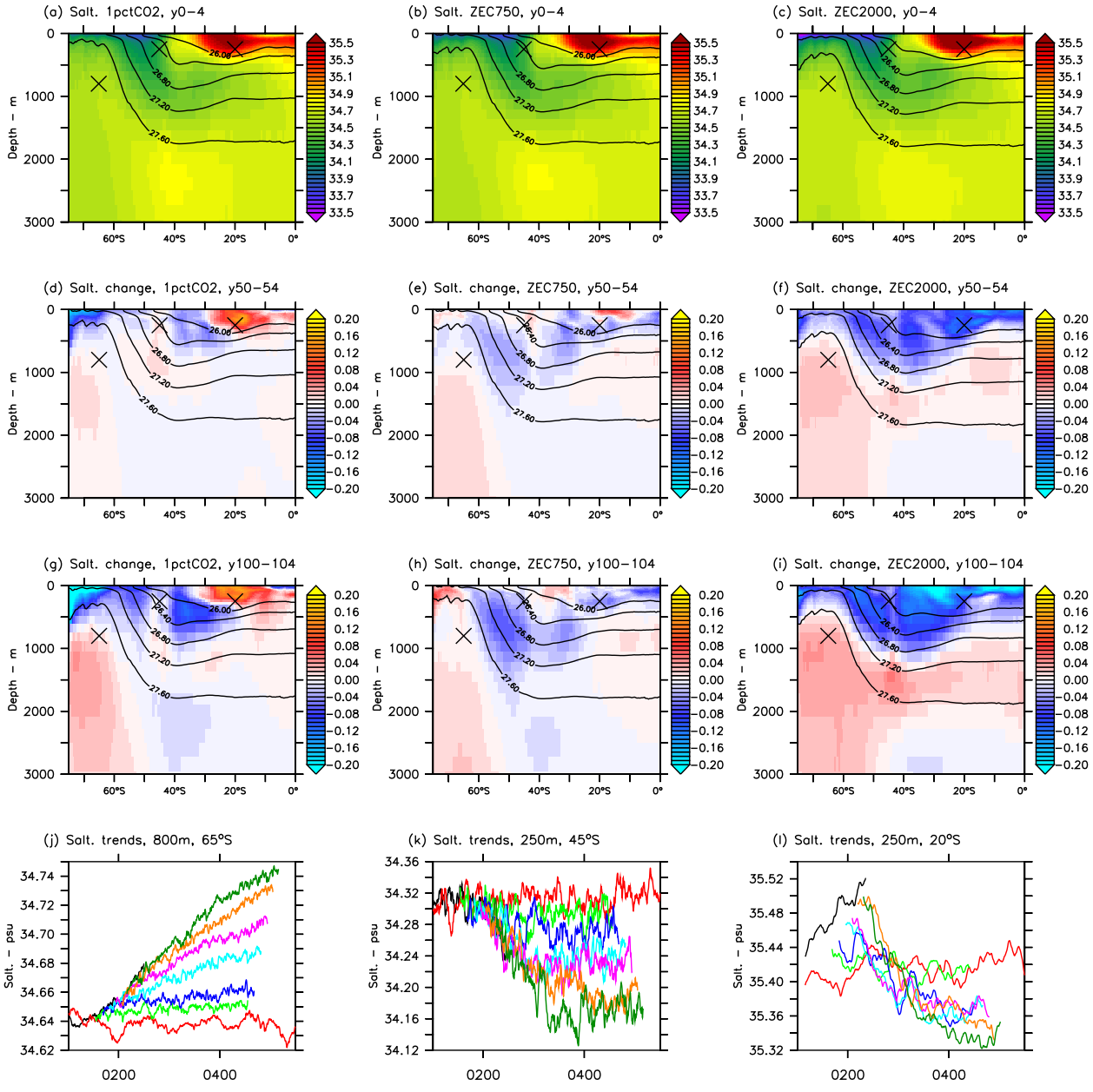

Figure 6. Changes and time series in average zonal sections of salinity, with the same layout as Fig. 5.

https://doi.org/10.5194/bg-2023-146
Preprint. Discussion started: 28 September 2023

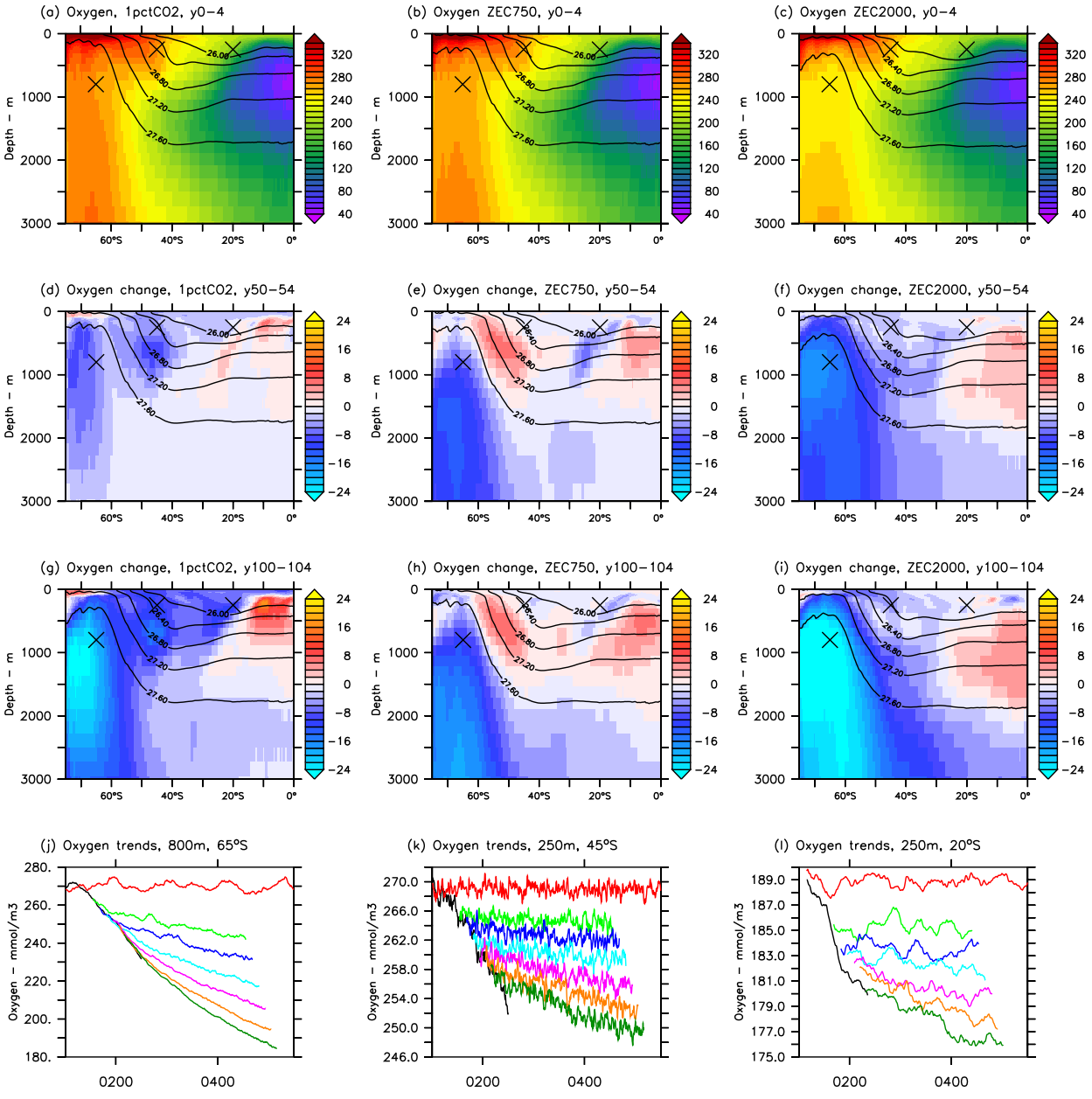

Figure 7. Changes and time series in average zonal sections of oxygen, with the same layout as Fig. 5.

https://doi.org/10.5194/bg-2023-146
Preprint. Discussion started: 28 September 2023

Biogeosciences
Discussions
Open Access
EGU

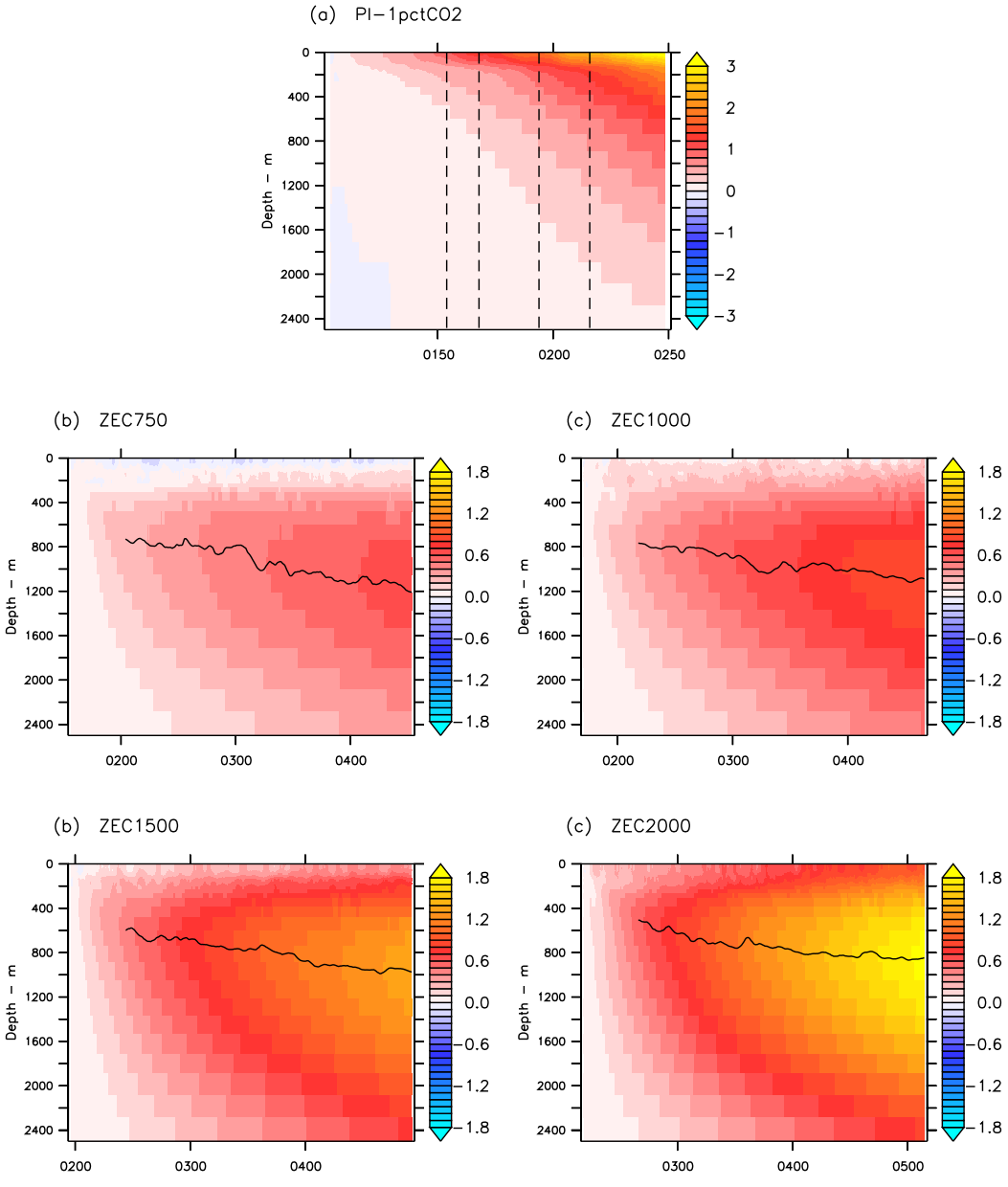

Figure 8. Heat uptake of the whole ocean as a function of depth and time, shown as changes in global averages of temperature within each experiment. Dashed vertical lines in panel (a) indicate the times that the ZEC experiments in (b)-(e) branch from the *1pctCO2*. Solid lines overlain indicate the depth of maximum change in temperature in ZEC branches.

https://doi.org/10.5194/bg-2023-146
Preprint. Discussion started: 28 September 2023

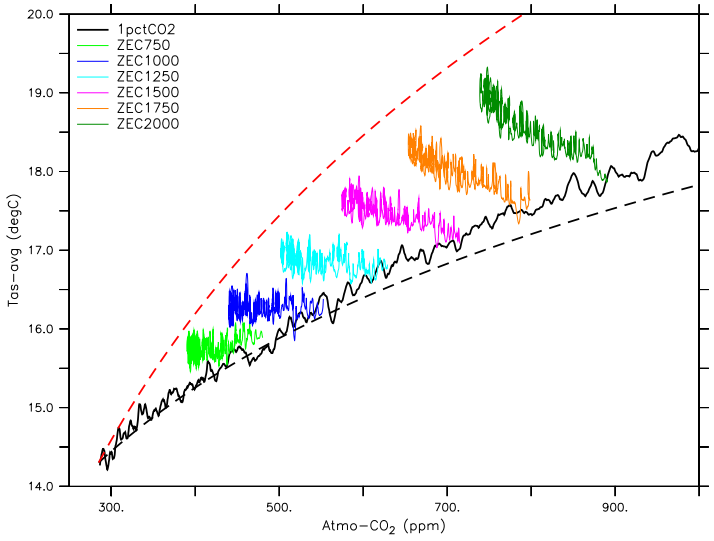

Figure 9. Time series of globally averaged surface temperature with respect to atmospheric CO_2 for the *1pctCO2* and ZEC branches. Dashed lines indicate temperatures corresponding to the transient climate response (black) and equilibrium climate sensitivity (red).

3.4 CO_2-temperature trajectories

Figure 9 shows the trajectories of *1pctCO2* and ZEC branches with respect to CO_2 and global average near-surface temperatures. The trajectories of these branches are consistent with climates approaching their equilibrium states after initial perturbations and warming in the *1pctCO2* experiment before branching. Overlying these experiments are temperatures corresponding to the Transient Climate Response (TCR) and Equilibrium Climate Sensitivity (ECS) of the ACCESS-ESM1.5, calculated with the logarithmic relationship of CO_2 and radiative or 'climate forcing' (Myhre et al., 1998) and assuming a constant climate feedback parameter (λ, Wm^{-2} $°C^{-1}$). Both TCR and ECS are expressed as the global warming associated with a doubling atmospheric CO_2, and TCR is typically substantially less than a models ECS. The TCR and ECS for the ACCESS-ESM1.5 are 1.95°C and 3.87°C respectively (Ziehn et al., 2020). The trajectory of *1pctCO2* in Fig. 9 starts from the lower left (285 ppm, 14.3°C) and moves to the right, generally following the TCR (the TCR is defined by the response of *1pctCO2* at 50 years). As ZEC experiments branch they turn left and move towards the ECS over the 300 years of integration. Consistent with the time series of the surface temperatures in Fig. 1, the trajectories of the lowest ZEC branches have stabilised near their equilibrium climates by the end of the 300-year integration and are close to ECS values. Climate states of higher ZEC branches are still evolving and with further model integration are expected to also stabilise at an equilibrium climate temperature, though this may take several centuries, or longer for the highest branches.

https://doi.org/10.5194/bg-2023-146
Preprint. Discussion started: 28 September 2023


Biogeosciences Discussions Open Access EGU

4 Analysis and Discussion

4.1 Climate inertia

As a way to explain and understand the global temperature trajectories in *1pctCO2* and ZEC branches, a simple model of independant slabs with different inertia, conceptually representing impacts from land and ocean, is used to replicate these trajectories. There are other simplified models that have been constructed to emulate full ESMs, such as "energy balance models" (e.g., Geoffroy et al., 2013), though the slab model based on temporal responses of the climate system is more than adequate to reproduce results from the ACCESS-ESM1.5. Global temperature is an average of just two slabs that both approach the same equilibrium temperature anomaly determined by time-evolving atmospheric CO_2, as diagnosed from ACCESS-ESM1.5 simulations, but each slab evolves with a different time constant. Various processes related to the heat uptake and response of surface temperature of both the land and the ocean are parameterised in the timescales assumed. These global temperature trajectories are shown in Fig. 10, where the timescale of the land slab is 1 year and effectively follows the equilibrium temperature while the ocean timescale is 300 years. See App. A for more details and discussion on the model setup. These timescales for land and ocean were determined by fitting to global temperatures of *1pctCO2*. The land and ocean have equal weight in this configuration in order that the trend of the slab model matches ACCESS-ESM1.5. Temperatures of slab models with ocean timescales of 100 and 500 years are also shown which over- and underestimate the temperature trends of the *1pctCO2* experiment. The slab model captures both the *1pctCO2* and the key trends of the ZECMIP trajectories shown, namely the slight decrease in *ZEC750*, neutral *ZEC1000* and increases in higher ZEC branches.

Being able to replicate the global temperatures with this slab model demonstrates that the ZEC trends found with ACCESS-ESM1.5 are due to the inertial response of the ocean within the climate system, which (from zonal pattern of Fig. 2) can largely be attributed to the Southern Ocean. In this way the Southern Ocean is like the "freight train" of the climate system. Once atmospheric CO_2 has been high enough, for long enough to start warming the Southern Ocean, it will continue warming and even affect the global climate. This global trajectory will not be corrected by zero-emission scenarios but rather require ongoing negative emissions, extracting CO_2 from the climate system.

Climate "tipping points" can be considered as positions at which the climate state no longer returns to its previous condition but rather continues evolving without applying further increases in climate forcing. This might be the case here, though the fanning out of global temperature trends in Fig. 1 indicate this does not occur at a single point as such, but rather it is a transition, where the later the branching off the *1pctCO2* experiment, or more CO_2 emitted before switching to a zero-emission trajectory, the stronger the ongoing warming in the climate state within the ZEC branch. Here, the Southern Ocean is not behaving as a tipping point exactly, though it does behave like one in the sense that the region is capable of driving ongoing changes to the climate system beyond the point where additional climate forcing is applied. This general result does not preclude other tipping points to be crossed in the process, notably changes to circulation and structure of the Southern Ocean during the warm epoch; for example, the point at which the average Antarctic sea ice area starts to decrease in Fig. 1f.

https://doi.org/10.5194/bg-2023-146
Preprint. Discussion started: 28 September 2023

Biogeosciences
Discussions
Open Access
EGU

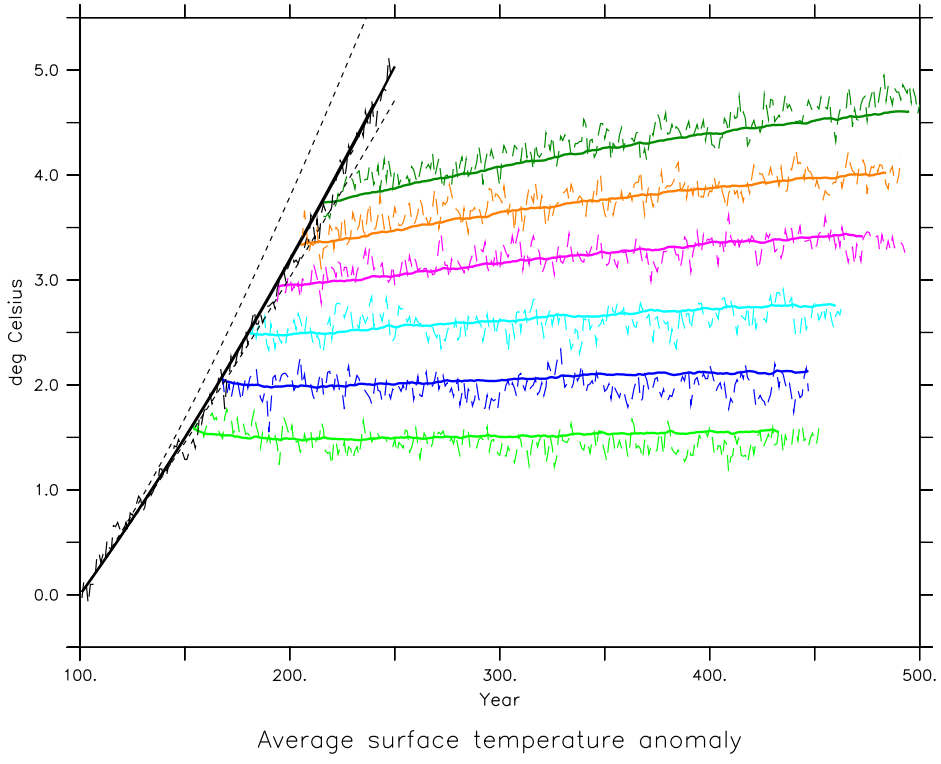

Figure 10. Global time series of average surface temperature for the *1pctCO2* and ZEC branches from ACCESS-ESM1.5 (dashed lines) and slab model (solid lines, same colour scheme as Fig. 9). Dotted black lines show slab model temperatures for *1pctCO2* with ocean time scales of 100 and 500 years.

4.2 Multi model Comparison

A curious observation from ZECMIP was the range of responses from the different models, such as in Fig. 6 of MacDougall et al. (2020). In particular, it was unclear why some models (ACCESS-ESM1.5 and the UKESM1-0-LL (Sellar et al., 2019)) showed positive ZEC values in *ZEC2000* while other models (CanESM5 (Swart et al., 2019), GFDL-ESM2M (Dunne et al., 2013) and MIROC-ES2L (Hajima et al., 2020)) were negative.

The slab model presented here, based on the ACCESS-ESM1.5 response, is now used to the assess how much these different multimodel ZEC responses reported are due to differences in the physical and biogeochemical components of these ESMs. Atmospheric CO_2 values diagnosed from each ZECMIP model, that have been made available at http://terra.seos.uvic.ca/ZEC (Eby, 2023), are used to force the slab model tuned to the ACCESS-ESM1.5 response and slab-model temperatures are com-

https://doi.org/10.5194/bg-2023-146
Preprint. Discussion started: 28 September 2023

pared to the temperatures from the original ZECMIP models that are also available. Figure 11 shows results of these comparisons for the three ESMs that submitted output for all three ZECMIP branches. The ECS of the slab model for these comparisons is made to match the ECS of each model as reported in MacDougall et al. (2020) and calculated again here in Table 2; with the one exception for the GFDL-ESM2M where a higher value of 2.9°C is used to approximately match the original *ZEC2000* temperatures instead of the reported 2.4°C. This is consistent with Paynter et al. (2018) who found the GFDL-ESM2M had a higher ECS in multi-millenial simulations due to changes in the climate feedback parameter associated with ongoing evolution is sea surface temperature and atmospheric state.

The first observation from Fig. 11 is the overall similarity of the response of the slab model with the temperatures found with original GFDL-ESM2M and UKESM results. In both of these models, the global temperatures in *ZEC2000* continue to rise on a centennial timescale, like the ACCESS-ESM1.5, despite the lower CO_2 values (Fig. 11a). This is in contrast to the different ZEC_{50} values from these models, as shown in Fig. 6 of the ZECMIP paper (MacDougall et al., 2020), and calculated again here (Table 2) where the UKESM were positive for all ZEC branches while GFDL-ESM2M were all negative. These disparate results can be associated with different responses at shorter, annual to decadal timescales.

The GFDL-ESM2M has the largest drawdown of CO_2 of the models shown (Fig. 11a) and there is cooling in both the original GFDL and slab models in the first decades of all ZEC branches (Fig. 11b). However, beyond 100 years, the centennial responses of the models dominate and temperatures rise in original GFDL-ESM2M results and the slab for *ZEC2000*. There is a similarity in the physical response of these two models in that there are similar relative trends in ZEC values for all branches in Table 2. The long term ZEC of the GFDL model is positive and increases like the original ACCESS-ESM1.5, despite different CO_2 responses.

In contrast, the UKESM has a relatively slow temperature response to the changing CO_2 even in the course of *1pctCO2* where the original UKESM temperature increases are apparently delayed with respect to the slab (Fig. 11d). This lagged response is also seen at the start of each ZEC branch, where temperatures continue increasing for the first decade, associated with the previous increasing CO_2 from before the branch points. Consequently, the ZEC_{50} calculated with UKESM is significantly positive, even for the lowest *ZEC750* branch which otherwise shows a relatively neutral response on the centennial timescales in both the original UKESM and slab results. Slab ZEC temperatures with the UKESM CO_2 that do not have this lagged response are negative for *ZEC750* and *ZEC1000*, and positive to *ZEC2000* whereas UKESM ZEC values are all positive (Table 2).

The MIROC ESM results are distinct to the other models here. The global temperatures in original MIROC results are decreasing on centennial timescales for all ZEC branches. The MIROC temperature response closely follows changes in CO_2 and climate forcing. In contrast, the slab tuned to the ACCESS-ESM1.5 has a slower response and shows rising temperatures in *ZEC2000* with the same MIROC CO_2. In Table 2, the ZEC_{50} values of the ACCESS slab are similar to the original MIROC ESM values, within ~ 0.1°C, whereas MIROC ESM ZEC_{200} values are 0.2 to 0.3°C lower than the ACCESS slab values.

From these comparisons, the many responses shown in ZECMIP models can largely be explained by the characteristics of the physical climate models with some influence of the carbon cycle on the decadal responses. Overall, ACCESS-ESM1.5, GFDL-ESM2M and UKESM are similar, showing significant responses at centennial timescales to changes in climate forcing which dominate long term temperature trends, in contrast to MIROC where temperatures follow the climate forcing relatively

https://doi.org/10.5194/bg-2023-146
Preprint. Discussion started: 28 September 2023

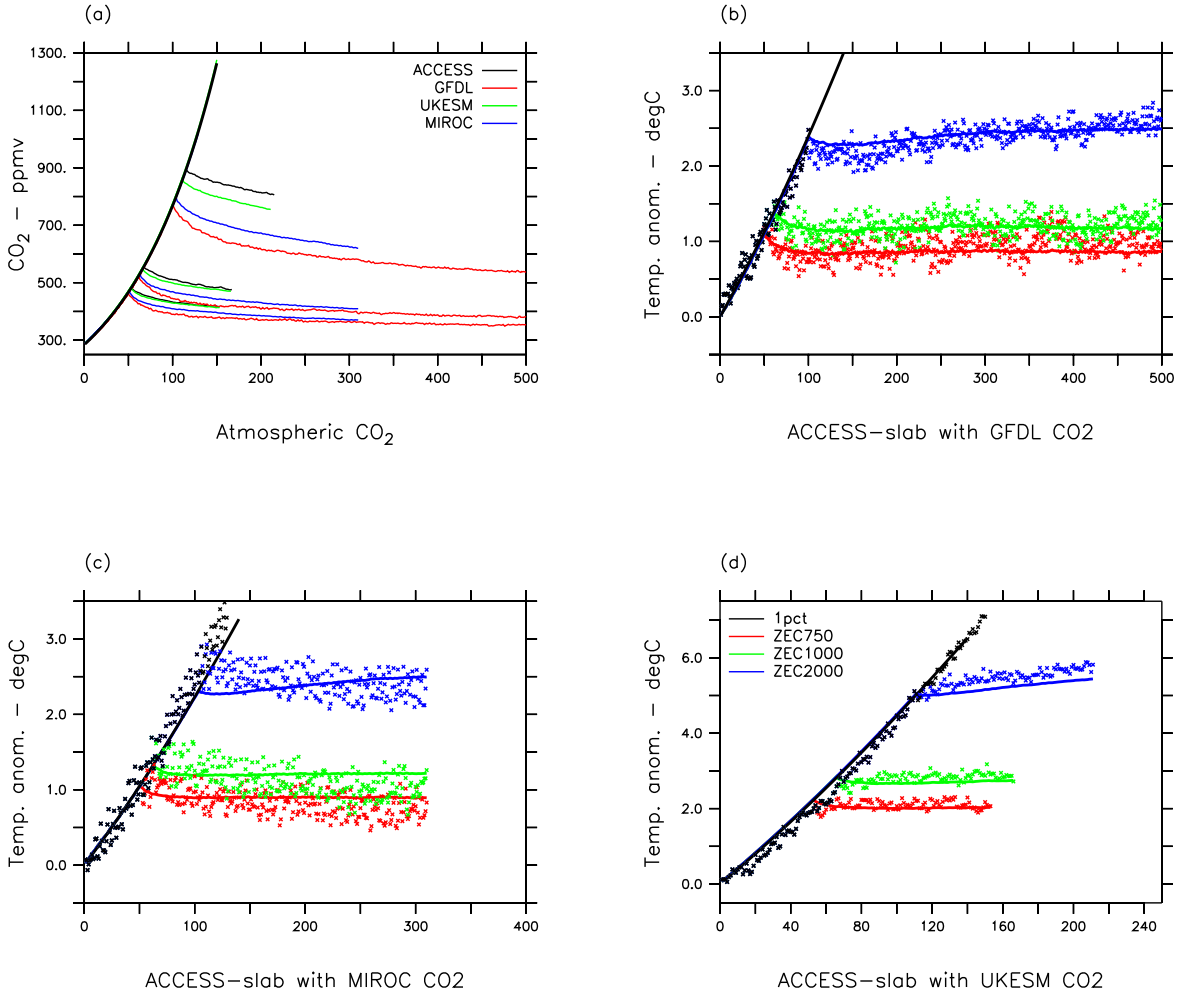

Figure 11. Global time series of (a) atmospheric CO_2 and average surface temperatures for the *1pctCO2* and ZEC branches from ESM models submitted to the ZECMIP: (b) GFDL, (c) MIROC and (d) UKESM. Annual averages of original model temperatures are shown as individual points, temperatures with the slab model are solid lines.

closely. Details in the physical response, such as the relative contributions at annual to decadal timescales, affect the values calculated for ZEC_{50}. The rapid CO_2 uptake of the GFDL-ESM2M lead to negative ZEC_{50} values in each branch whereas the lagged, decadal response in the UKESM produce positive ZEC_{50} values. These observations indicate that while ZEC_{50} values are relevant on policy timescales, where modifications to current rates of CO_2 emissions may modify the expected ZEC_{50}, this

https://doi.org/10.5194/bg-2023-146
Preprint. Discussion started: 28 September 2023

Biogeosciences Discussions Open Access EGU

Table 2. ZEC values from ZECMIP model temperatures submitted to MacDougall et al. (2020), as well as ZEC values from the ACCESS-ESM1.5 slab with CO_2 diagnosed from ZECMIP models. Values are the differences between 20-year averages centred at the year of the ZEC branch (or 10-year average in the case of UKESM ZEC_{100} values), relative to the 20-year average from the respective *1pctCO2* centred at the branch point.

		ZEC_{50}		ZEC_{100}		ZEC_{200}	
		Original	Slab	Original	Slab	Original	Slab
GFDL	*ZEC750*	-0.33	-0.26	-0.25	-0.26	-0.29	-0.24
	ZEC1000	-0.29	-0.25	-0.13	-0.25	-0.02	-0.20
	ZEC2000	-0.11	-0.06	+0.02	-0.01	+0.22	+0.11
MIROC	*ZEC750*	-0.17	-0.19	-0.24	-0.18	-0.36	-0.19
	ZEC1000	-0.05	-0.16	-0.23	-0.15	-0.36	-0.14
	ZEC2000	-0.08	-0.03	-0.13	+0.05	-0.23	+0.15
UKESM	*ZEC750*	+0.11	-0.29	+0.03	-0.27	n/a	n/a
	ZEC1000	+0.28	-0.21	+0.26	-0.16	n/a	n/a
	ZEC2000	+0.53	+0.12	+0.78	+0.33	n/a	n/a

metric can be a poor representation of the complete response of ESMs and longer ZEC values are useful to consider for long term implications to the climate state.

In the case of the ACCESS-ESM1.5, the temporal evolution of zonal average temperatures, as shown in Fig. 2, clearly indicate the latitudes of the Southern Ocean as regions of a lagged response in *1pctCO2* and also ongoing warming in all ZEC branches tested; Fig. 12 is an equivalent plot of zonal average temperatures with available ZECMIP ESMs, namely MIROC-ES2L, the UKESM1-0-LL and ACCESS-ESM1.5. Note, these results are based on the experiments originally submitted to ZECMIP and available on the ESGF (World Climate Research Program, 2023), including the original ACCESS-ESM1.5 results submitted. In the transient *1pctCO2* phase (left column), the broad patterns in the temperature changes are similar, each model shows greatest warming in the Arctic and slowest warming around the Southern Ocean, though Arctic warming is greater in the UKESM by several degrees. There is an overall global neutral response in the 100 years of *ZEC750* for ACCESS-ESM1.5 and UKESM, and cooling in MIROC (middle column), and temperature changes related to slow modes of climate variability are evident. ACCESS-ESM1.5 showed warming at Southern Ocean latitudes in *ZEC750* before in Fig. 2, but this manifests on timescales longer than the 100 years shown here. In *ZEC750*, the Arctic region cools in MIROC but continues to warm in UKESM. In *ZEC2000* (right column), consistent with Fig. 11, there is broad warming in ACCESS-ESM1.5 and UKESM, but cooling in MIROC. The Southern Ocean features prominently as a region of ongoing warming in both ACCESS-ESM1.5 and UKESM, particularly at latitudes under the influence of sea ice, south of 60° S. The Arctic in the UKESM shows less warming than the ACCESS-ESM1.5 in *ZEC2000*, though the UKESM has warmed more here in the transient experiment before branching. Even in MIROC, which shows overall cooling in *ZEC2000*, the Southern Ocean is a site of local warming, in

https://doi.org/10.5194/bg-2023-146
Preprint. Discussion started: 28 September 2023

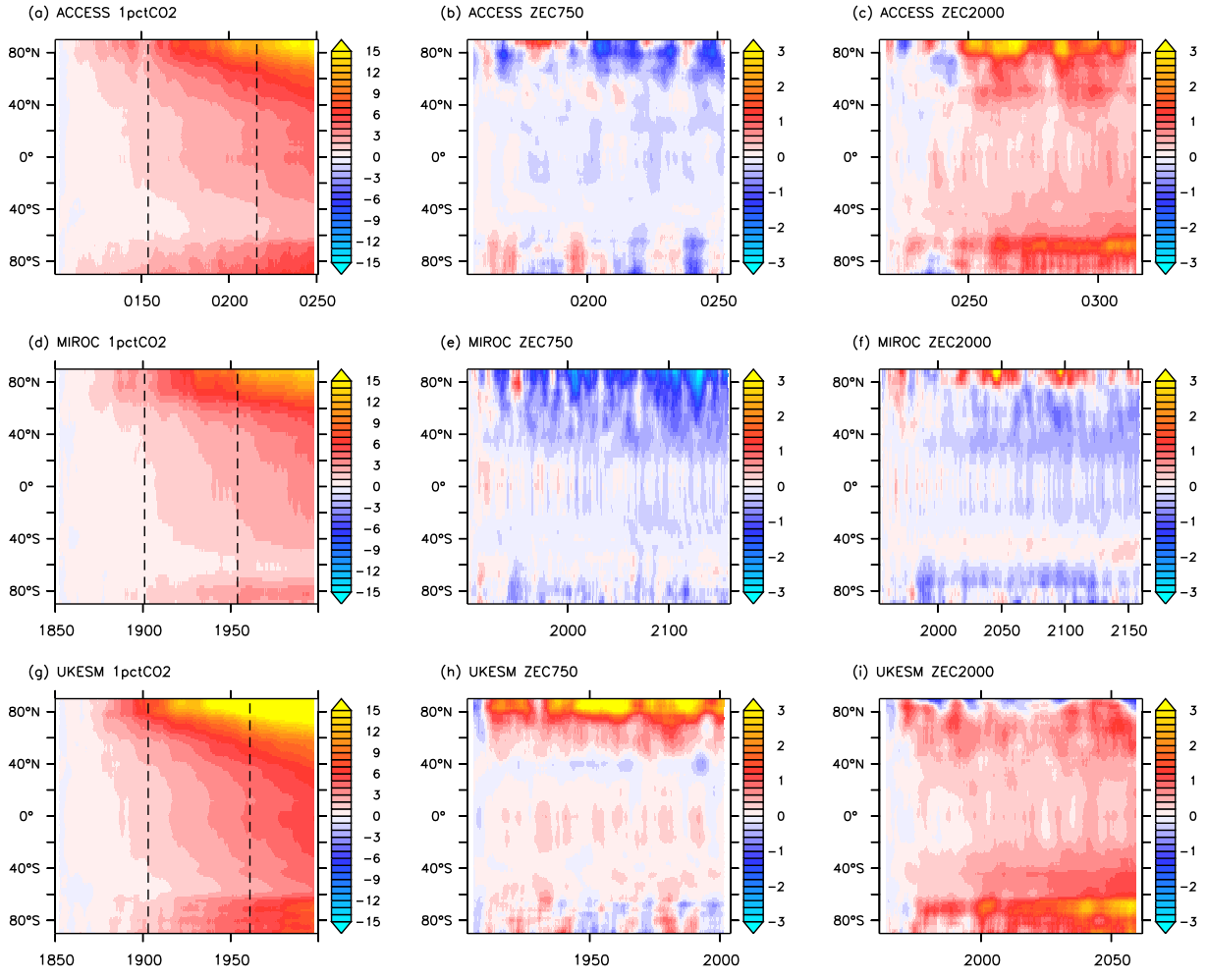

Figure 12. Changes in zonal average temperatures in *1pctCO2* (left), *ZEC750* (middle) and *ZEC2000* (right) from ZECMIP ESM models: ACCESS-ESM1.5 (top), MIROC (centre) and UKESM (bottom). Zonal temperatures are also smoothed by averaging over 5 years, and are differenced with respect to the first 10 years of each experiment. Branch times of each *ZEC750* and *ZEC2000* are indicated by dashed lines in their respective *1pctCO2* parent.

this case at latitudes predominantly outside seasonal sea ice, 40–60° S; demonstrating that the response of the Southern Ocean to continue warming in high ZEC branches is common in all full ESMs.

The biogeochemical component and its carbon cycle still play a role in the trajectory of temperature in ZEC scenarios. For instance, the CO_2 uptake in all other ZECMIP models is more rapid than in ACCESS-ESM1.5 (panel a, Fig. 11) especially in the case of the GFDL-ESM2M, and the slab ZEC_{50} and ZEC_{100} values in Table 2 are all less than the values for the same branch in Table 1. In higher ZEC branches, the CO_2 is still significantly higher than preindustrial values for all models and

https://doi.org/10.5194/bg-2023-146
Preprint. Discussion started: 28 September 2023

the slow component drove increasing temperatures in the long term for most models except MIROC (Fig. 11). The ACCESS slab temperatures increase in all cases of high ZEC branches, even when driven by CO_2 from MIROC, clearly demonstrating a different physical response between ACCESS-ESM1.5 and MIROC in the long term.

5 Conclusions

The ACCESS-ESM1.5 submission to the recent ZECMIP (MacDougall et al., 2020), was one of only two full-ESMs that demonstrated significant positive ZEC values, or ongoing warming, in the branch that switched to a zero-emission scenario after emitting 2000 Pg of carbon, the *ZEC2000* branch. In contrast, ZEC has been assumed to be about neutral for the present day climate state. Extra experiments with ACCESS-ESM1.5 have been executed to better understand the processes behind this ongoing warming in the climate, with more branch points after the emission of intermediate carbon budgets and also longer climate integrations up to 300 years with zero emissions.

The rates of ongoing global temperature increases vary smoothly across the ZEC branches, the increase is greatest on branches after the emission of the most carbon, and global temperature decreases slightly for the lowest branch, *ZEC750*. Longer integrations demonstrate significant regional changes that were not apparent in the original ZECMIP integrations. For instance, even in *ZEC750* there is a decline in Antarctic sea ice that is apparent after ∼200 years. Zonal time series of surface temperatures show that while the Southern Ocean is slow to warm in the transient *1pctCO2* experiment, this is the region that continues to warm in all ZEC branches, even in low ZEC branches and regardless of the global response.

Clear and persistent changes are evident in the subsurface ocean that start in the *1pctCO2* and do not recover in any of the ZEC branches. The decrease in the overturning circulation is associated with a decrease in density of the southernmost waters. These circulation changes then drive ongoing changes in the distribution of ocean tracers, both physical and biogeochemical. Heat increases at depth, even in low branches where there is cooling in surface waters. Biogeochemical responses are affected by changing circulation and changing source/sink terms. Oxygen decreases in the deep Southern Ocean in all branches with the decrease in overturning, but also increases locally at positions where reduced ocean productivity reduces consumption of subsurface oxygen.

The evolution of ZEC branches with respect to atmospheric CO_2 and average surface temperature all traverse the space between the Transient Climate Responce (as followed by the *1pctCO2*) and the Equilibrium Climate Sensitivity. In this space, the ECS is significantly higher than the TCR, so it is actually quite reasonable for a climate to be warming even with decreasing CO_2 and climate forcing while the climate states traverses from a transient response towards its equilibrium state.

Global trajectories found with the full ACCESS-ESM1.5 are well reproduced with a simple composite slab model, where each slab approaches the same equilibrium temperature change prescribed by the climate forcing with a different timescale. The ongoing temperature increases are explained by the slow response of the ocean. The Southern Ocean in particular behaves as the “freight train” of the climate system; once the Southern Ocean starts warming significantly it will take large change in the climate forcing, such as a substantial reduction in CO_2 beyond the natural uptake of land and ocean, in order to reverse its temperature trajectory and its affect on the global climate.

https://doi.org/10.5194/bg-2023-146
Preprint. Discussion started: 28 September 2023


Biogeosciences Discussions Open Access EGU

370 *Data availability.*

CMIP6 output from the ACCESS-ESM1.5 experiments, and from other models that submitted results to the original ZECMIP analysis, is freely available through the Earth System Grid Federation (World Climate Research Program, 2023), including the *piControl*, the *1pctCO2* and the original branch experiments submitted to ZECMIP: *ZEC750*, *ZEC1000* and *ZEC2000*. CO_2 values from ZECMIP models used to drive the ACCESS slab model were obtained from the ZECMIP data repository (Eby, 375 2023). For output related to the extra branches described in the manuscript, please contact the authors.

Appendix A: Slab model

In Section 4.1, time series in global temperature are compared with a simple model (Fig. 10) composed of slabs with different "thermal inertia," or slabs that respond to changes in climate forcing on different timescales. This slab model is also driven with results from other ZECMIP models (Fig. 11). In this slab model, the temperature of each independant slab (T_i) tends towards 380 the equilibrium temperature (T_{eq}) that is a function of atmospheric CO_2 with a prescribed timescale (τ_i),

$$\frac{dT_i}{dt} = \left(T_{eq}(CO_2) - T_i\right)/\tau_i \tag{A1}$$

The global temperature is then a weighted average of the slabs ($T_{av} = (\sum_i w_i T_t)/\sum_i w_i$). These temperatures are anomalies with respect to preindustrial conditions.

The equilibrium temperature is determined by the equilibrium climate sensitivity (T_{ECS}, the change in equilibrium temper- 385 ature with a doubling of atmospheric CO_2 from preindustrial, CO_2^{PI}, diagnosed with the method described in Gregory et al., 2004) and the atmospheric CO_2 diagnosed from ACCESS-ESM1.5 experiments, or other ZECMIP ESMs. All other climate forcing terms (e.g. aerosols and non-CO_2 greenhouse gases) in these experiments are held constant at preindustrial values. Climate forcing, or radiative forcing perturbations in Wm^{-2}, is proportional to the logarithm of atmospheric CO_2 (Myhre et al., 1998), so the equilibrium temperature can be determined from

$$T_{eq}(CO_2) = T_{ECS}\frac{\ln(CO_2/CO_2^{PI})}{\ln(2)} \tag{A2}$$

Table A1 describes the slabs used here to replicate the ACCESS-ESM1.5 global temperature time series in Fig. 10. The idealised "slab" model is intentionally kept simple while replicating the global trends from ACCESS-ESM1.5, and here two slabs are found to meet this objective. The two slabs used conceptually correspond to the response the land and ocean to changes, as indicated. The timescale of the "land"' response (τ=1) effectively means the land follows the equilibrium temperature here. 395 Note, the land weighting of 0.5 is significantly higher than the areal fraction of land over the real Earth. However, there is no intent to interpret these slabs to represent actual land temperatures, rather just their influence on the global temperature. Also, for the "ocean" slab only a single τ is applied when in reality different regions of the ocean will respond differently to changes in climate forcing (such as the well-mixed Southern Ocean relative to the stratified tropics), and the single value represents a blended response of these varying oceanic components balanced with the terrestrial response.

https://doi.org/10.5194/bg-2023-146
Preprint. Discussion started: 28 September 2023


Biogeosciences Discussions Open Access EGU

Table A1. Components of the slab model in presented in Fig. 10.

Slab	Fraction	ECS °C	Timescale years
Land	0.5	3.87	1
Ocean	0.5	3.87	300

Other processes could be considered in the construction of this slab model, such as heat exchange between the slabs and/or the additional of extra slabs (a slab with a decadal timescale for example). However, given that the two-slab model effectively reproduces the temperature time series in Fig. 10 these options are considered not necessary for the purposes used here.

To produce the trends of ZEC branches shown in Fig. 10 and 11, each T_i starts from a temperature anomaly of 0°C, or the preindustrial state, and evolves along the trajectory defined by the CO_2 from the *1pctCO2* to the branch point, where it then tends towards the temperatures determined by the atmospheric CO_2 diagnosed from ACCESS-ESM1.5 or ZECMIP model experiments for each ZEC branch.

Author contributions.

TZ, MC and RL contributed to the development of the model. TZ ran experiments. MC analysed output and prepared the manuscript, all authors provided comments.

Competing interests.

The authors declare that they have no conflict of interest.

Acknowledgements. This research used computation resources and archives available at the National Computational Infrastructure (NCI), which is located at the Australian National University and supported by the Australian Government.

MC, TZ and RL receive funding from the Australian Government under the National Environmental Science Program (NESP).

https://doi.org/10.5194/bg-2023-146
Preprint. Discussion started: 28 September 2023

References

Dunne, J. P., John, J. G., Shevliakova, E., Stouffer, R. J., Krasting, J. P., Malyshev, S. L., Milly, P. C. D., Sentman, L. T., Adcroft, A. J., Cooke, W., Dunne, K. A., Griffies, S. M., Hallberg, R. W., Harrison, M. J., Levy, H., Wittenberg, A. T., Phillips, P. J., and Zadeh, N.: GFDL's ESM2 Global Coupled Climate–Carbon Earth System Models. Part II: Carbon System Formulation and Baseline Simulation Characteristics*, Journal of Climate, 26, 2247 – 2267, https://doi.org/10.1175/JCLI-D-12-00150.1, 2013.

Eby, M.: Zero Emissions Commitment Model Intercomparison Project, Globally averaged data and EMIC data repository, University of Victoria, available at: http://terra.seos.uvic.ca/ZEC, last access 2 July 2023., 2023.

Eyring, V., Bony, S., Meehl, G. A., Senior, C. A., Stevens, B., Stouffer, R. J., and Taylor, K. E.: Overview of the Coupled Model Intercomparison Project Phase 6 (CMIP6) experimental design and organization, Geosci. Model Dev., 9, 1937–1958, doi:10.519/gmd-9-1937-2016, 2016.

Geoffroy, O., Saint-Martin, D., Olivié, D. J. L., Voldoire, A., Bellon, G., and Tytéca, S.: Transient Climate Response in a Two-Layer Energy-Balance Model. Part I: Analytical Solution and Parameter Calibration Using CMIP5 AOGCM Experiments, Journal of Climate, 26, 1841 – 1857, https://doi.org/https://doi.org/10.1175/JCLI-D-12-00195.1, 2013.

Gregory, J. M., Ingram, W. J., Palmer, M. A., Jones, G. S., Stott, P. A., Thorpe, R. B., Lowe, J. A., Johns, T. C., and Williams, K. D.: A new method for diagnosing radiative forcing and climate sensitivity, Geophysical Research Letters, 31, https://doi.org/https://doi.org/10.1029/2003GL018747, 2004.

Griffies, S. M.: Elements of MOM5, GFDL Ocean Group Technical Report No. 7, NOAA/Geophysical Fluid Dynamics Laboratory, p. Code and documentation available online at www.gfdl.noaa.gov., 2012.

Hajima, T., Watanabe, M., Yamamoto, A., Tatebe, H., Noguchi, M. A., Abe, M., Ohgaito, R., Ito, A., Yamazaki, D., Okajima, H., Ito, A., Takata, K., Ogochi, K., Watanabe, S., and Kawamiya, M.: Development of the MIROC-ES2L Earth system model and the evaluation of biogeochemical processes and feedbacks, Geoscientific Model Development, 13, 2197–2244, https://doi.org/10.5194/gmd-13-2197-2020, 2020.

Hunke, E. C. and Lipscomb, W. H.: CICE: The Los Alamos sea ice model documentation and software user's manual, Version 4.1, LA-CC-06-012, Los Alamos National Laboratory, N. M., 2010.

Jones, C. D., Frölicher, T. L., Koven, C., MacDougall, A. H., Matthews, H. D., Zickfeld, K., Rogelj, J., Tokarska, K. B., Gillett, N. P., Ilyina, T., Meinshausen, M., Mengis, N., Séférian, R., Eby, M., and Burger, F. A.: The Zero Emissions Commitment Model Intercomparison Project (ZECMIP) contribution to C4MIP: quantifying committed climate changes following zero carbon emissions, Geoscientific Model Development, 12, 4375–4385, https://doi.org/10.5194/gmd-12-4375-2019, 2019.

Kowalczyk, E. A., Stevens, L., Law, R. M., Dix, M., Wang, Y. P., Harman, I. N., Haynes, K., Srbinovsky, J., Pak, B., and Ziehn, T.: The land surface model component of ACCESS: description and impact on the simulated surface climatology, Aus. Meteor. Oceanogr. J., 63, 65–82, 2013.

Law, R. M., Ziehn, T., Matear, R. J., Lenton, A., Chamberlain, M. A., Stevens, L. E., Wang, Y.-P., Srbinovsky, J., Bi, D., Yan, H., and Vohralik, P. F.: The carbon cycle in the Australian Community Climate and Earth System Simulator (ACCESS-ESM1) – Part 1: Model description and pre-industrial simulation, Geoscientific Model Development, 10, 2567–2590, https://doi.org/10.5194/gmd-10-2567-2017, 2017.

MacDougall, A. H., Frölicher, T. L., Jones, C. D., Rogelj, J., Matthews, H. D., Zickfeld, K., Arora, V. K., Barrett, N. J., Brovkin, V., Burger, F. A., Eby, M., Eliseev, A. V., Hajima, T., Holden, P. B., Jeltsch-Thömmes, A., Koven, C., Mengis, N., Menviel, L., Michou,

M., Mokhov, I. I., Oka, A., Schwinger, J., Séférian, R., Shaffer, G., Sokolov, A., Tachiiri, K., Tjiputra, J., Wiltshire, A., and Ziehn, T.: Is there warming in the pipeline? A multi-model analysis of the Zero Emissions Commitment from CO_2, Biogeosciences, 17, 2987–3016, https://doi.org/10.5194/bg-17-2987-2020, 2020.

Mackallah, C., Chamberlain, M. A., Law, R. M., Dix, M., Ziehn, T., Bi, D., Bodman, R., Brown, J. R., Dobrohotoff, P., Druken, K., Evans, B., Harman, I. N., Hayashida, H., Holmes, R., Kiss, A. E., Lenton, A., Liu, Y., Marsland, S., Meissner, K., Menviel, L., O'Farrell, S., Rashid, H. A., Ridzwan, S., Savita, A., Srbinovsky, J., Sullivan, A., Trenham, C., Vohralik, P. F., Wang, Y.-P., Williams, G., Woodhouse, M. T., and N., Y.: ACCESS datasets for CMIP6: methodology and idealised experiments, Journal of Southern Hemisphere Earth Systems Science, https://doi.org/10.1071/ES21031, 2022.

Matthews, H. D. and Weaver, A. J.: Committed climate warming, Nature Geoscience, 3, 142–143, https://doi.org/10.1038/ngeo813, 2010.

Myhre, G., Highwood, E. J., Shine, K. P., and Stordal, F.: New estimates of radiative forcing due to well mixed greenhouse gases, Geophysical Research Letters, 25, 2715–2718, https://doi.org/10.1029/98GL01908, 1998.

Oke, P. R., Griffin, D. A., Schiller, A., Matear, R. J., Fiedler, R., Mansbridge, J., Lenton, A., Cahill, M., Chamberlain, M. A., and Ridgway, K.: Evaluation of a near-global eddy-resolving ocean model, Geoscientific Model Development, 6, 591–615, https://doi.org/10.5194/gmd-6-591-2013, 2013.

Paynter, D., Frölicher, T., Horowitz, L., and Silvers, L.: Equilibrium Climate Sensitivity Obtained from Multi-Millennial Runs of Two GFDL Climate Models, Journal of Geophysical Research: Atmospheres, 123, https://doi.org/10.1002/2017JD027885, 2018.

Rogelj, J., Shindell, D., Jiang, K., Fifita, S., Forster, P., Ginzburg, V., Handa, C., Kheshgi, H., Kobayashi, S., Kriegler, E., Mundaca, L., Séférian, R., and Vilariño, M. V.: Mitigation Pathways Compatible with 1.5°C in the Context of Sustainable Development, p. 93–174, Cambridge University Press, https://doi.org/10.1017/9781009157940.004, 2018.

Rogelj, J., Forster, P. M., Kriegler, E., Smith, C. J., and Séférian, R.: Estimating and tracking the remaining carbon budget for stringent climate targets, Nature, 571, 335–342, https://doi.org/10.1038/s41586-019-1368-z, 2019.

Sellar, A. A., Jones, C. G., Mulcahy, J. P., Tang, Y., Yool, A., Wiltshire, A., O'Connor, F. M., Stringer, M., Hill, R., Palmieri, J., Woodward, S., de Mora, L., Kuhlbrodt, T., Rumbold, S. T., Kelley, D. I., Ellis, R., Johnson, C. E., Walton, J., Abraham, N. L., Andrews, M. B., Andrews, T., Archibald, A. T., Berthou, S., Burke, E., Blockley, E., Carslaw, K., Dalvi, M., Edwards, J., Folberth, G. A., Gedney, N., Griffiths, P. T., Harper, A. B., Hendry, M. A., Hewitt, A. J., Johnson, B., Jones, A., Jones, C. D., Keeble, J., Liddicoat, S., Morgenstern, O., Parker, R. J., Predoi, V., Robertson, E., Siahaan, A., Smith, R. S., Swaminathan, R., Woodhouse, M. T., Zeng, G., and Zerroukat, M.: UKESM1: Description and Evaluation of the U.K. Earth System Model, Journal of Advances in Modeling Earth Systems, 11, 4513–4558, https://doi.org/https://doi.org/10.1029/2019MS001739, 2019.

Swart, N. C., Cole, J. N. S., Kharin, V. V., Lazare, M., Scinocca, J. F., Gillett, N. P., Anstey, J., Arora, V., Christian, J. R., Hanna, S., Jiao, Y., Lee, W. G., Majaess, F., Saenko, O. A., Seiler, C., Seinen, C., Shao, A., Sigmond, M., Solheim, L., von Salzen, K., Yang, D., and Winter, B.: The Canadian Earth System Model version 5 (CanESM5.0.3), Geoscientific Model Development, 12, 4823–4873, https://doi.org/10.5194/gmd-12-4823-2019, 2019.

The HadGEM2 Development Team:, Martin, G. M., Bellouin, N., Collins, W. J., Culverwell, I. D., Halloran, P. R., Hardiman, S. C., Hinton, T. J., Jones, C. D., McDonald, R. E., McLaren, A. J., O'Connor1, F. M., Roberts, M. J., Rodriguez, J. M., Woodward, S., Best, M. J., Brooks, M. E., Brown, A. R., Butchart, N., Dearden, C., Derbyshire, S. H., Dharssi, I., Doutriaux-Boucher, M., Edwards, J. M., Falloon, P. D., Gedney, N., Gray, L. J., Hewitt, H. T., Hobson, M., Huddleston, M. R., Hughes, J., Ineson, S., Ingram, W. J., James, P. M., Johns, T. C., Johnson, C. E., Jones, A., Jones, C. P., Joshi, M. M., Keen, A. B., Liddicoat, S., Lock, A. P., Maidens, A. V., Manners, J. C., Milton, S. F., Rae, J. G. L., Ridley, J. K., Sellar, A., Senior, C. A., Totterdell, I. J., Verhoef, A., Vidale, P. L., and Wiltshire, A.: The HadGEM2

https://doi.org/10.5194/bg-2023-146
Preprint. Discussion started: 28 September 2023

490 family of Met Office Unified Model climate configurations, Geosci. Model Dev., 4, 723–757, https://doi.org/10.5194/gmd-4-723-2011, 2011.

World Climate Research Program: Coupled Model Intercomparison Project, Phase 6, United States Department of Energy, available at: https://esgf-node.llnl.gov/projects/cmip6/, last access 23 May 2023., 2023.

Ziehn, T., Chamberlain, M. A., Law, R., Lenton, A., Bodman, R. W., Dix, M., Stevens, L., Wang, Y. P., and Srbinovsky, J.: The Australian
495 Earth System Model: ACCESS-ESM1.5, J. Southern Hemis. Earth Sys. Sci., 70, 193–214, https://doi.org/10.1071/ES19035, 2020.

Ziehn, T., Wang, Y. P., and Huang, Y.: Land carbon-concentration and carbon-climate feedbacks are significantly reduced by nitrogen and phosphorus limitation, Environmental Research Letters, 16, 074043, https://doi.org/10.1088/1748-9326/ac0e62, 2021.